

**Nagra**

Nationale  
Genossenschaft  
für die Lagerung  
radioaktiver Abfälle

**Cédra**

Société coopérative  
nationale  
pour l'entreposage  
de déchets radioactifs

**Cisra**

Società cooperativa  
nazionale  
per l'immagazzinamento  
di scorie radioattive



# TECHNICAL REPORT 89-13

## SUBCRITICAL CRACK GROWTH IN HOT-ISOSTATICALLY POSTCOMPACTED HIGH-GRADE ALUMINA

T. Fett<sup>1)</sup>  
W. Hartlieb<sup>1)</sup>  
K. Keller<sup>2)</sup>  
D. Munz<sup>1) 3)</sup>  
W. Rieger<sup>4)</sup>

APRIL 1989

<sup>1)</sup> Kernforschungszentrum Karlsruhe,  
Institut für Material- und Festkörperforschung IV

<sup>2)</sup> Universität Karlsruhe,  
Institut für Keramik im Maschinenbau

<sup>3)</sup> Universität Karlsruhe,  
Institut für Zuverlässigkeit und Schadenskunde im Maschinenbau

<sup>4)</sup> Metoxit AG Thayngen/Switzerland



**Nagra**

Nationale  
Genossenschaft  
für die Lagerung  
radioaktiver Abfälle

**Cédra**

Société coopérative  
nationale  
pour l'entreposage  
de déchets radioactifs

**Cisra**

Società cooperativa  
nazionale  
per l'immagazzinamento  
di scorie radioattive

# TECHNICAL REPORT 89-13

## SUBCRITICAL CRACK GROWTH IN HOT-ISOSTATICALLY POSTCOMPACTED HIGH-GRADE ALUMINA

T. Fett<sup>1)</sup>  
W. Hartlieb<sup>1)</sup>  
K. Keller<sup>2)</sup>  
D. Munz<sup>1) 3)</sup>  
W. Rieger<sup>4)</sup>

APRIL 1989

<sup>1)</sup> Kernforschungszentrum Karlsruhe,  
Institut für Material- und Festkörperforschung IV

<sup>2)</sup> Universität Karlsruhe,  
Institut für Keramik im Maschinenbau

<sup>3)</sup> Universität Karlsruhe,  
Institut für Zuverlässigkeit und Schadenskunde im Maschinenbau

<sup>4)</sup> Metoxit AG Thayngen / Switzerland

**Der vorliegende Bericht wurde im Auftrag der Nagra erstellt. Die Autoren haben ihre eigenen Ansichten und Schlussfolgerungen dargestellt. Diese müssen nicht unbedingt mit denjenigen der Nagra übereinstimmen.**

**Le présent rapport a été préparé sur demande de la Cédra. Les opinions et conclusions présentées sont celles des auteurs et ne correspondent pas nécessairement à celles de la Cédra.**

**This report was prepared as an account of work sponsored by Nagra. The viewpoints presented and conclusions reached are those of the author(s) and do not necessarily represent those of Nagra.**

### Abstract

The subcritical crack-growth behaviour of natural cracks in a hot isostatically post-compacted high-grade alumina ceramic was tested in a concentrated salt solution at 70 °C. The result of static bending tests yielded a crack-growth law that can be described by a power law with an exponent  $n=73.5$ . This high value reflects an excellent resistance to subcritical crack growth. A comparison with  $Al_2O_3$ -materials investigated earlier has been included.

### Kurze Zusammenfassung

Das Verhalten des unterkritischen Risswachstums natürlicher Risse in einer hochwertigen, gesinterten und anschliessend heissisostatisch nachverdichteten Aluminiumoxydkeramik wurde in einer konzentrierten Salzlösung bei 70 °C untersucht. Aus den Ergebnissen statischer Biegeversuche konnte ein Risswachstumsgesetz abgeleitet werden, wonach das Risswachstum als Potenzgesetz mit einem Exponenten  $n=73,5$  beschrieben werden kann. Dieser hohe Wert weist auf einen ausgezeichneten Widerstand gegen unterkritisches Risswachstum hin. Das eingesetzte Material wird mit den im Rahmen früherer Arbeiten untersuchten  $Al_2O_3$ -Materialien verglichen.

### Résumé succinct

On a étudié à 70 °C dans une solution saline concentrée le comportement de la croissance sous-critique de fissures dans une céramique d'alumine de haute qualité postcompactée isostatiquement à haute température après le frittage. Des résultats d'essais de flexion statiques, on peut conclure que la croissance des fissures peut être décrite par une loi de puissance avec un exposant  $n=73,5$ . Cette valeur élevée implique une excellente résistance à la croissance sous-critique de fissures. Le matériau utilisé est comparé aux aluminés testées dans le cadre d'études antérieures.

# SUBCRITICAL CRACK GROWTH IN HOT-ISOSTATICALLY POSTCOMPACTED HIGH-GRADE ALUMINA

## 1. Introduction

Alumina is being considered for the ultimate storage of high-level waste as a candidate container material. It shows subcritical crack growth with a crack growth rate

$$\frac{da}{dt} = v(K_I) \quad (1)$$

where  $K_I$  is the stress intensity factor

$$K_I = \sigma Y \sqrt{a} \quad (2)$$

$\sigma$  denotes the stress and  $a$  the depth of a crack in a structure and  $Y$  is a geometric correction factor dependent on the shape of the crack and the component. Very often the crack growth can be described by a power law

$$v = AK_I^n = A^*(K_I/K_{Ic})^n \quad (3)$$

where  $A$  and  $n$  represent crack growth parameters and  $K_{Ic}$  is the fracture toughness. To ensure a high resistance to subcritical crack growth, the exponent  $n$  in eq.(1) should be very high. In a first investigation [1] the qualification of a hot isostatically pressed alumina (Asea, Sweden) was assessed by determination of crack growth in synthetic water which is representative of groundwaters in the granitic bedrock of Northern Switzerland. Strong crack growth with a very low crack growth exponent  $n \approx 20$  was found as the main result. In a second report [2] the same analysis was made for an alternative alumina provided by Metoxit AG, Thayngen (Switzerland). A markedly higher exponent  $n \approx 50$  was determined.

In this paper, results are reported on an alumina provided by Metoxit AG (Switzerland), which in contrast to the material investigated in [2] had been subjected to hot-isostatic postcompaction.

## 2. Manufacturing procedure

The starting material used was identical to that as described in report 87-09. It was a commercial 99.9%  $\text{Al}_2\text{O}_3$  produced by Metoxit AG, CH-8240 Thayngen. The material was provided by NAGRA. The main contaminations of the raw material were determined to be:

MgO	400 ppm	(grain refiner)
SiO <sub>2</sub>	30 ppm	
Fe <sub>2</sub> O <sub>3</sub>	15 ppm	
CaO	5 ppm	
Na <sub>2</sub> O	40 ppm	
K <sub>2</sub> O	1 ppm	
Cr <sub>2</sub> O <sub>3</sub>	1 ppm	
TiO <sub>2</sub>	1 ppm	

The raw material had an average grain size ( $d_{50}$ ) of  $0.5\mu\text{m}$  and a BET of  $7\text{ m}^2/\text{g}$ . It was used as spray-dried. The material was isopressed on an automatic isopress in the shape of cylindrical rods and sintered at a temperature of  $1550^\circ\text{C}$ . After sintering the rods were inspected for cracks with a penetration method based on ultraviolet fluorescence (Zyglo test). Subsequently, the rods were subjected to a HIP (hot isostatic pressing) post compaction, at a temperature of  $1450^\circ\text{C}$  and under a pressure of 1000 bar in argon. After the HIP process, the rods were again inspected for flaws; bars of  $4.4\times 4.4\times 50\text{mm}$  were cut out of the rods and the surface was diamond ground and subsequently polished on three sides. The density was determined by the Archimedes method as  $3.975\text{ g/cm}^3$ , this corresponds to 99.6% TD. Grain size was determined on polished and etched surfaces of representative samples. The grain size was measured using the intersecting line method as  $3.25\mu\text{m}$ . In fig.1 and 2, polished (x100) and etched (x500) micrographs of the alumina samples are presented.

### 3. Experimental investigations

The method of determining the subcritical crack growth law is based on measurements of the strength in an inert environment and measurements of lifetimes in a static bending test performed in the real environment. The method is described in detail in [1]-[4].

#### 3.1 Dynamic bending strength

Before testing, the alumina specimens were annealed for 4 hours in a  $1 \cdot 10^{-5}$  bar vacuum at 1150°C. To determine the inert bending strength  $\sigma_c$ , 25 specimens were subjected to dynamic 4-point bending tests in air with a 20mm inner span and a 40mm outer span. The tests were performed at a very high loading rate of 3000N/s - using a transient recorder - to avoid any subcritical crack propagation. In fig.3 the Weibull representation of the inert strength data is shown. Application of the *maximum-likelihood method* yielded the parameters

$$m = 10.0 \quad \sigma_0 = 383 \text{ MPa}$$

The fracture toughness obtained with Chevron-notched specimens was  $K_{Ic} = 3.8 \text{ MPa}\sqrt{\text{m}}$

#### 3.2 Lifetime measurements

A salt solution specified by NAGRA was used as the test environment. The concentrations in mg/l were

NaCl	8297
KCl	86
MgCl <sub>2</sub> · 6H <sub>2</sub> O	22
SrCl <sub>2</sub> · 6H <sub>2</sub> O	64
NaF	8
NaHCO <sub>3</sub>	84
CaCl <sub>2</sub> · 2H <sub>2</sub> O	3191
Na <sub>2</sub> SO <sub>4</sub>	2307

identical to those used in [1]. In that environment static bending tests were performed at 70°C and with bending stresses of 230MPa and 253MPa. The lifetimes  $t_f$  obtained with these stresses have been plotted in fig.4 in a Weibull representation.

### 3.3 Results

From the strength  $\sigma_c$  and lifetimes  $t_f$  the crack growth rates can be determined using the relation

$$v(K_{II}) = - \frac{2}{t_f \sigma_c^2} \left( \frac{K_{Ic}}{Y_i} \right)^2 \frac{d[\log(K_{II}/K_{Ic})]}{d[\log(t_f \sigma^2 Y_i^2)]} \quad (4)$$

The lifetime quantity  $t_f \sigma^2$  was calculated from the measurements and plotted in fig.5 versus  $\sigma/\sigma_c$  for corresponding failure probabilities. The mean curve is given by the straight line. From these data the subcritical crack growth rate was computed applying eq.(4). The geometric function for small surface cracks with an assumed semi-circular shape is  $Y = 1.13 \cdot 2/\sqrt{\pi}$ . Figure 6 shows the result as a  $v$ - $K_I$ -curve. It can be seen that for the whole range of crack growth rates the  $v$ - $K_I$ -curve can be expressed by a power law with  $A = 7 \cdot 10^{-41}$  (in: MPa,m,s) and  $n = 73.5$ . An integration of the power law yields the well-known lifetime formula for a constant load test as

$$t_f = B \sigma_c^{n-2} \sigma^{-n} \quad (5)$$

with

$$B = \frac{2}{A Y^2 (n-2) K_{Ic}^{n-2}} \quad (6)$$

Equation (5) is appropriate to make lifetime predictions. Since the crack sizes in ceramics are statistically distributed, this prediction yields a lifetime distribution, which is given by

$$t_f = B \sigma_0^{n-2} \sigma^{-n} \exp \left[ \frac{n-2}{m} \ln \ln \frac{1}{1-F} \right] \quad (7)$$

In fig.7 this equation is plotted as solid lines for the experimentally obtained values of  $B$ ,  $n$  and  $m = 10$  and  $\sigma_0 = 383$ MPa. The dashed lines represent the material investigated in [1] and the dashed-dotted lines express on the results obtained in [2]. For containers suitable for ultimate storage an admissible failure probability  $F = 0.001$  is assumed. Two points are of interest:

1. A minimum lifetime of 1000 years may be required. Which are the admissible tensile stresses? Insertion of  $F = 1 \cdot 10^{-3}$ ,  $n = 73.5$ ,  $m = 10$ ,  $B = 8.4 \cdot 10^{-4}$  MPa<sup>2</sup>h,  $\sigma_0 = 383$ MPa and  $t_f = 8.76 \cdot 10^6$  h gives

$$\sigma_{\max} = 109 \text{ MPa}$$

2. In the container residual stresses  $\sigma_{res}$  caused in fabrication are supposed. The expected lifetimes are

- for  $\sigma_{res} = 100\text{MPa}$        $t_f = 4.7 \cdot 10^5$  years
- for  $\sigma_{res} = 120\text{MPa}$        $t_f = 0.7$  years

These examples have been entered in fig.7

The lifetime predictions mentioned in this chapter are valid for parts of approximately the same sizes as the specimens tested. It is known that the strength and the lifetime will decrease if the volumes and surfaces of real components are larger than those of measured bending specimens. Consequently, the tolerable stresses and attainable lifetimes diminish. The distribution of stresses in the container wall has to be known to allow exact calculations to be made.

#### *4. Discussion and comparison with earlier results*

To give a comparison with the materials tested earlier, all  $v$ - $K_I$ -curves are plotted in fig.8 . Since the fracture toughness data are nearly identical ( $\approx 4 \text{ MPa}\sqrt{\text{m}}$ ), the curves can be directly compared in this representation. It is obvious that the alumina investigated in this report is characterised by a significantly higher exponent  $n$  which is very important for lifetime predictions. From the point of view of subcritical crack growth the material investigated seems to be best qualified for long-term application as a container material. The variation of the crack growth exponent  $n$  has to be interpreted as a function of compositional and microstructural properties of the materials investigated. Impurities such as  $\text{SiO}_2$ ,  $\text{Na}_2\text{O}$ ,  $\text{CaO}$  and other oxides forming glassy phases in the grain boundaries are of influence on the  $n$ -value, as well as microstructural features such as grain size and density which determine the mechanical properties. Generally, strength is increased with decreasing grain size, with decreasing volume fraction of porosity, and with the shape of pores and flaws, angular pores being more harmful than rounded pores. The influence of a glassy phase on the mechanical properties can not be as clearly defined, because the glassy phase also can modify porosity content and shape. Small concentrations of second phase can strengthen the material, whereas large concentrations can be detrimental. In a corrosive environment, crack propagation will be enhanced by the presence of impurities in the crack pit. From the results obtained in the investigation of three materials with varying density/porosity and microstructure it can be concluded that the crack propagation exponent  $n$  is reduced with increasing content of impurities (99.7 vs. 99.9%  $\text{Al}_2\text{O}_3$ ), grain size (9 vs. 3  $\mu\text{m}$ ), and density (3.90 vs. 3.97  $\text{g}/\text{cm}^3$ ). These statements are, however, rather qualitative and cannot, at

(3.90 vs. 3.97 g/cm<sup>3</sup>). These statements are, however, rather qualitative and cannot, at present, give a quantitative explanation of the n-value obtained. On the other hand, they can be used as guidelines for the production of an alumina material which is subjected to high stresses in corrosive environment at elevated temperatures for prolonged time. From the data obtained, a recommendation can be made as follows:

- high purity raw material (over 99.9% Al<sub>2</sub>O<sub>3</sub>)
- low temperature sintering to obtain small grain size
- HIP postcompaction to reduce pore/ flaw size and to obtain non-angular pores.

Comparison with literature data can only be made omitting the influence of the composition of the corrosive aqueous medium and of temperature. If one accepts these shortcomings, the data for n obtained in this work show an acceptable agreement with data for n-values obtained by Dalgleish and Rawlings [5] and by Fett and Munz [6] for different aluminas of varying purity, composition and structural as well as mechanical properties. A comparison of data is given in Table 1. In order to clarify the influence of the nature of the corrosive medium and of temperature it will be necessary to extend the investigation by subjecting identical materials to test conditions with varying temperatures (20/70 °C) and nature of the corrosive medium (distilled water/ salt solution).

## 5. Summary

The subcritical crack growth of a hot-isostatically postcompacted high grade alumina in a highly concentrated salt solution at 70°C was investigated by lifetime measurements in static bending tests. The most important results are:

- The Weibull parameters of the inert bending strength distribution for the material investigated were found to be
 
$$m = 10.0, \sigma_0 = 383 \text{ MPa}$$
- The v-K<sub>I</sub>-curve obtained can be expressed by a power law with an exponent n=73.5. This high value implies an excellent crack growth resistance.
- The high-purity alumina investigated in this study is superior to the hot isostatically pressed alumina of [1] and also superior to the material studied in [2], at least for long term applications. Comparison with the results obtained on the latter material shows in particular the improvement that can be achieved by hot-isostatic postcompaction.

- The crack growth results are compared with that of other high pure  $\text{Al}_2\text{O}_3$ -ceramics tested by the authors in earlier investigations. The high resistance against subcritical crack growth found in the present investigation is in accordance with these literature data, although in the present paper the test conditions were more serious.
- The high n-values obtained for natural cracks are not unusual for high purity  $\text{Al}_2\text{O}_3$ . Whilst the materials IV and V (mentioned in Table 1) were tested in water at room temperature, it is shown by material III that even under severe test conditions (aggressive environment, and elevated temperature) a high resistance against subcritical crack growth is obtainable.

## 6. References

- [1] T. Fett, K. Keller, D. Munz, "Determination of crack growth parameters of alumina in 4-point bending tests", NAGRA Technical Report 85-51, Sept. 1985.
- [2] T. Fett, W. Hartlieb, K. Keller, D. Munz, "Subcritical crack growth in high-grade alumina for container applications" NAGRA Technical Report 87-09, Sept. 1987.
- [3] T. Fett, D. Munz, "Determination of  $v$ - $K_I$ -curves by a modified evaluation of lifetime measurements in static bending tests", Commun. of the Amer. Ceram Soc. 68,(1985) C213-C215.
- [4] T. Fett, K. Keller, D. Munz, "Determination of  $v$ -K curves for subcritical crack growth in naturally cracked specimens", cfi/Ber. DKG 64(1987),433-439.
- [5] B.J. Dalgleish, R.D. Rawlings "A comparison of the mechanical behavior of aluminas in air and simulated body environments" J. of Biomedical Materials Research 15(1981),527-542.
- [6] T. Fett, D. Munz, "Time-to-failure in static bending tests on  $Al_2O_3$  with natural and artificial surface cracks" cfi/Ber. DKG 61(1984),446-453.

		Mat. I ASEA	Mat. II Metoxit	Mat. III Metoxit	Mat. IV Feld- mühle	Mat. V Feld- mühle
manufacturing technique		HIP	sintered	sintered + HIP post com- pacted	not spe- cified	not spe- cified
density	g/cm <sup>3</sup>	-	3.90	3.975	3.92	3.90
average grain size	μm	-	4	3.25	3-4	2.7-3.8
medium		salt solu- tion	salt solu- tion	salt solu- tion	distilled water	distilled water
temperature	°C	70	70	70	20	20
inert bending strength	MPa	369	430	383	296	333
m		10.4	9.7	10	14	7.7
$K_{Ic}$	MPa√m	4.0	3.9	3.8	-	-
n		20	48	73.5	52	69
Reference		[1]	[2]	this investi- gation	[6]	[6]

Table 1. Comparison of the aluminas

## 7. Figures

Fig.1 Micrograph of a polished specimen (x100).

Fig.2 Micrograph of an etched specimen (x500).

Fig.3 Weibull-plot of the inert bending strength  $\sigma_c$ .

Fig.4 Lifetimes in 4-point bending tests in salt solution at 70°C.

Fig.5 Lifetime quantity  $t_f \sigma^2$  as a function of "normalised stress"  $\sigma/\sigma_c$ .

Fig.6  $v$ - $K_I$ -curve obtained from eq.(4).

Fig.7 Nomograph for lifetime predictions:

(solid line: this investigation);

(dashed lines: material investigated in [1]);

(dashed-dotted lines: material investigated in [2]).

Fig.8 Comparison of subcritical crack growth behaviour of the competing aluminas.

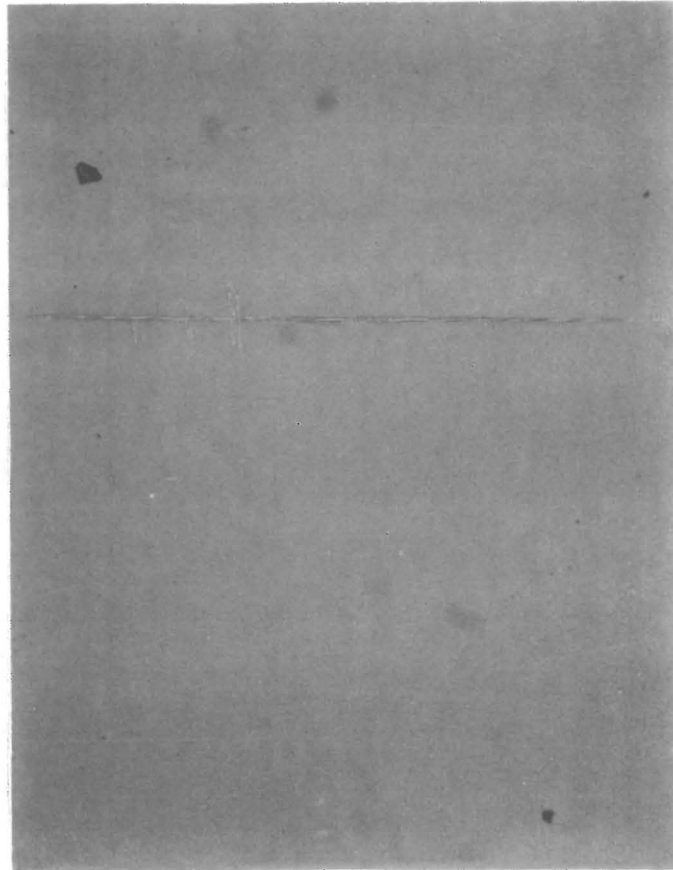


Fig.1 Micrograph of a polished specimen (x100).

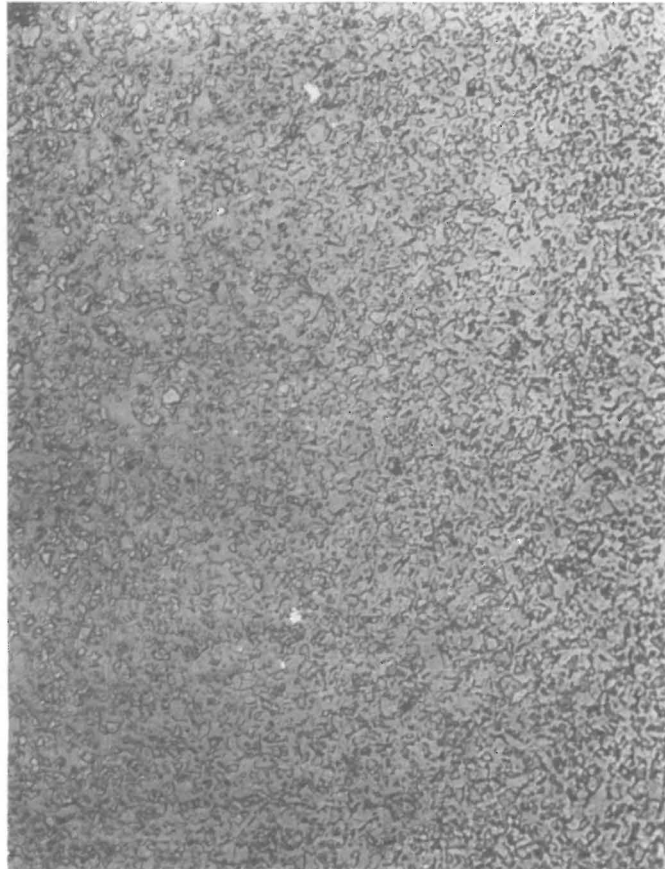


Fig.2 Micrograph of an etched specimen (x500).

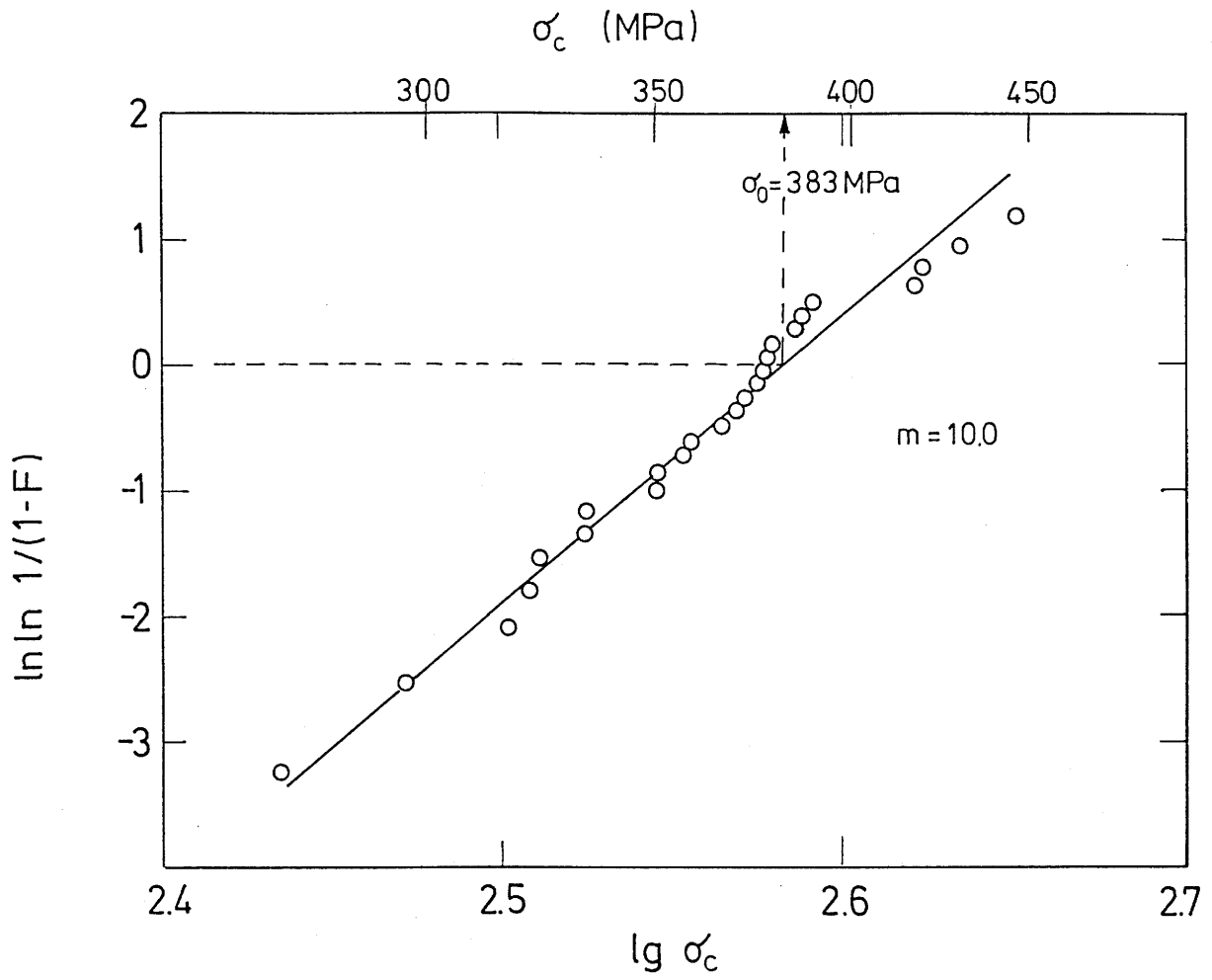


Fig.3 Weibull-plot of the inert bending strength  $\sigma_c$ .

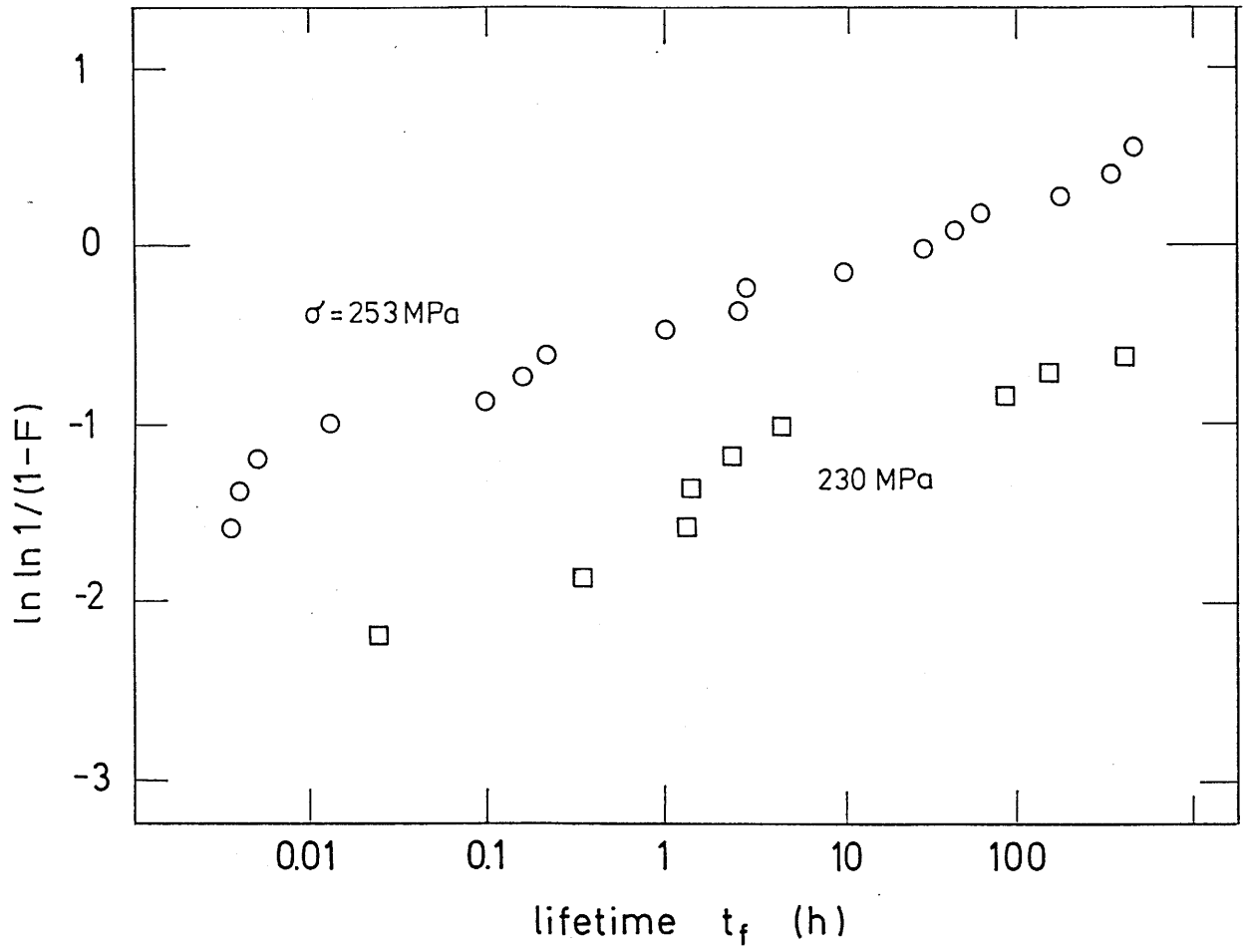


Fig.4 Lifetimes in 4-point bending tests in salt solution at 70°C.

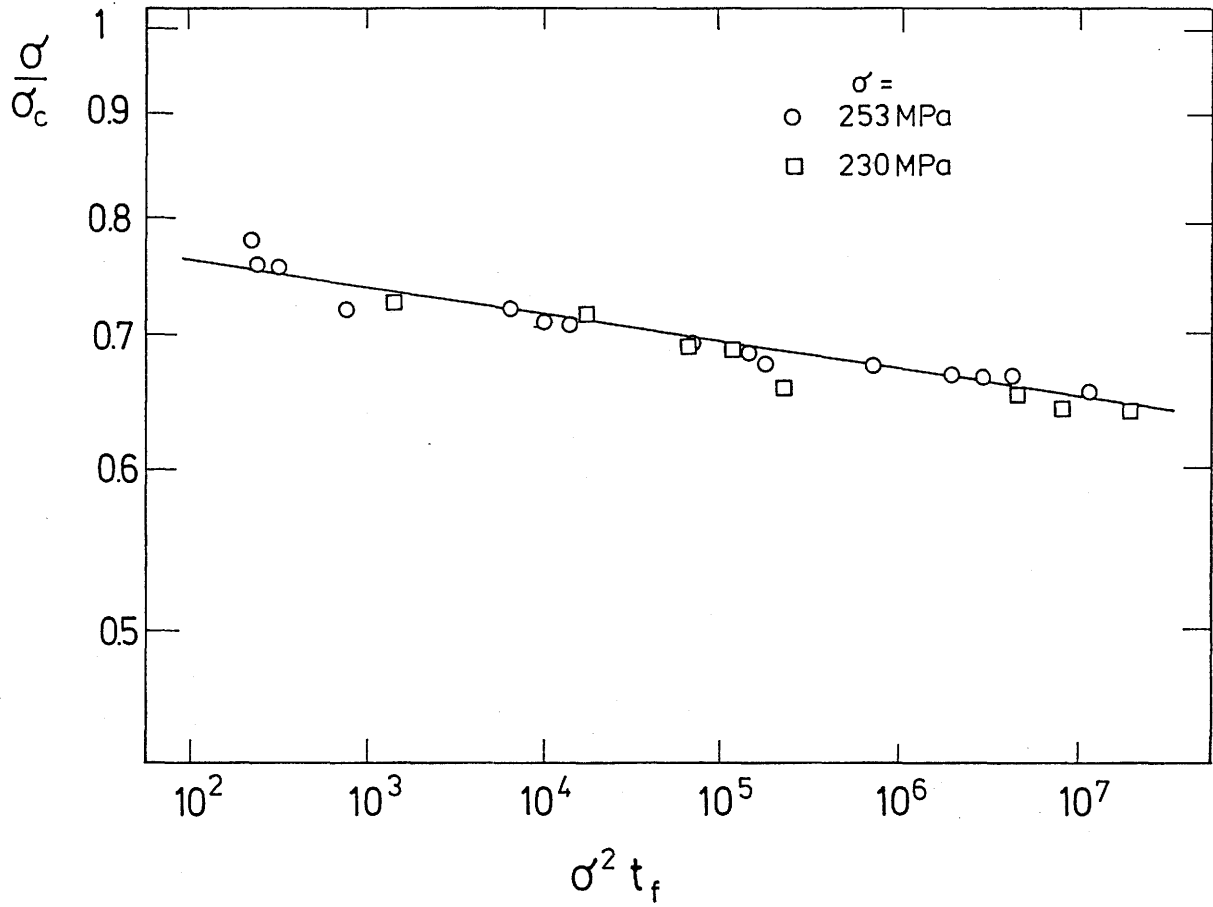


Fig.5 Lifetime quantity  $t_f \sigma^2$  as a function of "normalised stress"  $\sigma / \sigma_c$ .

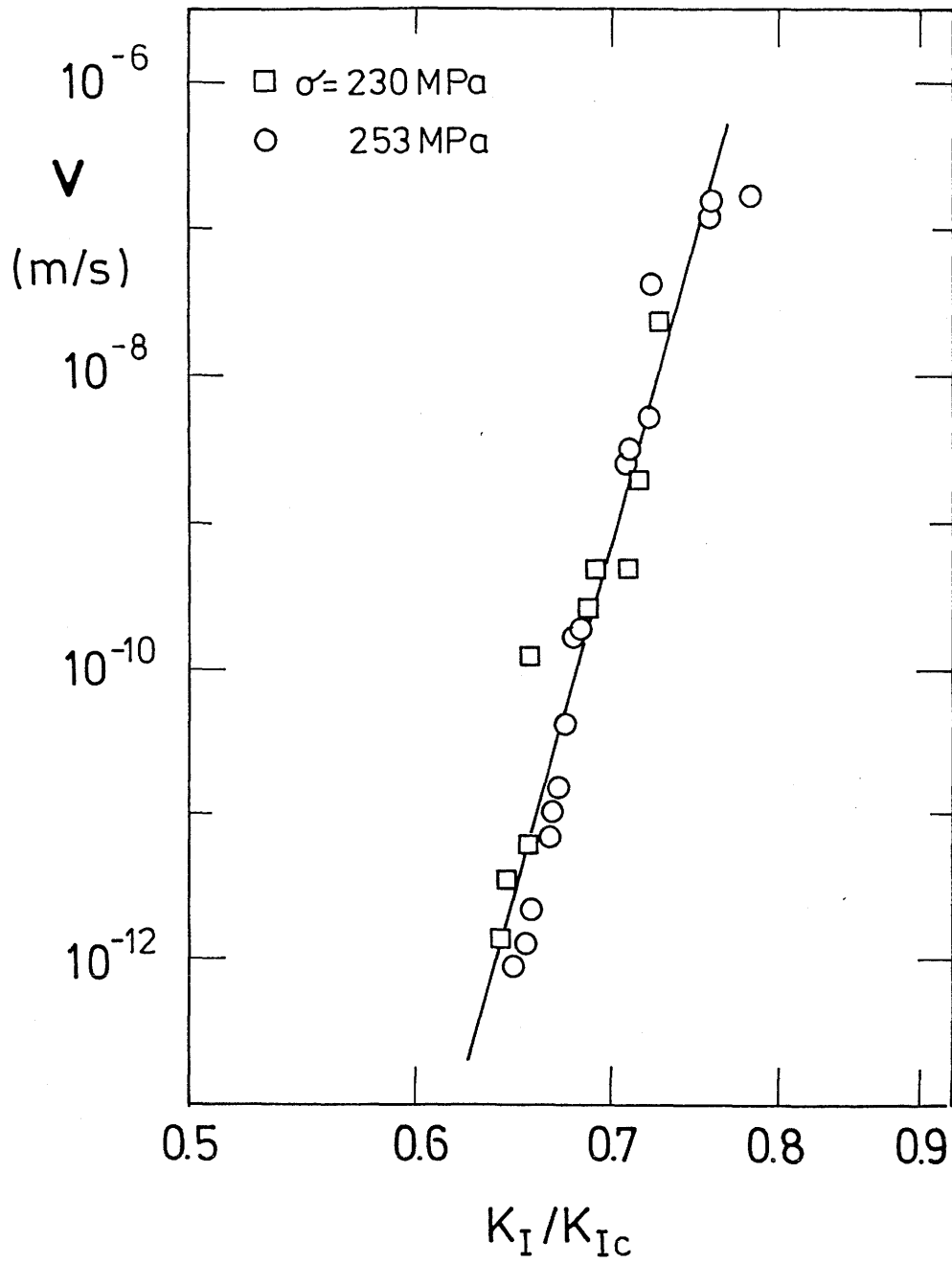


Fig.6  $v$ - $K_I$ -curve obtained from eq.(4).

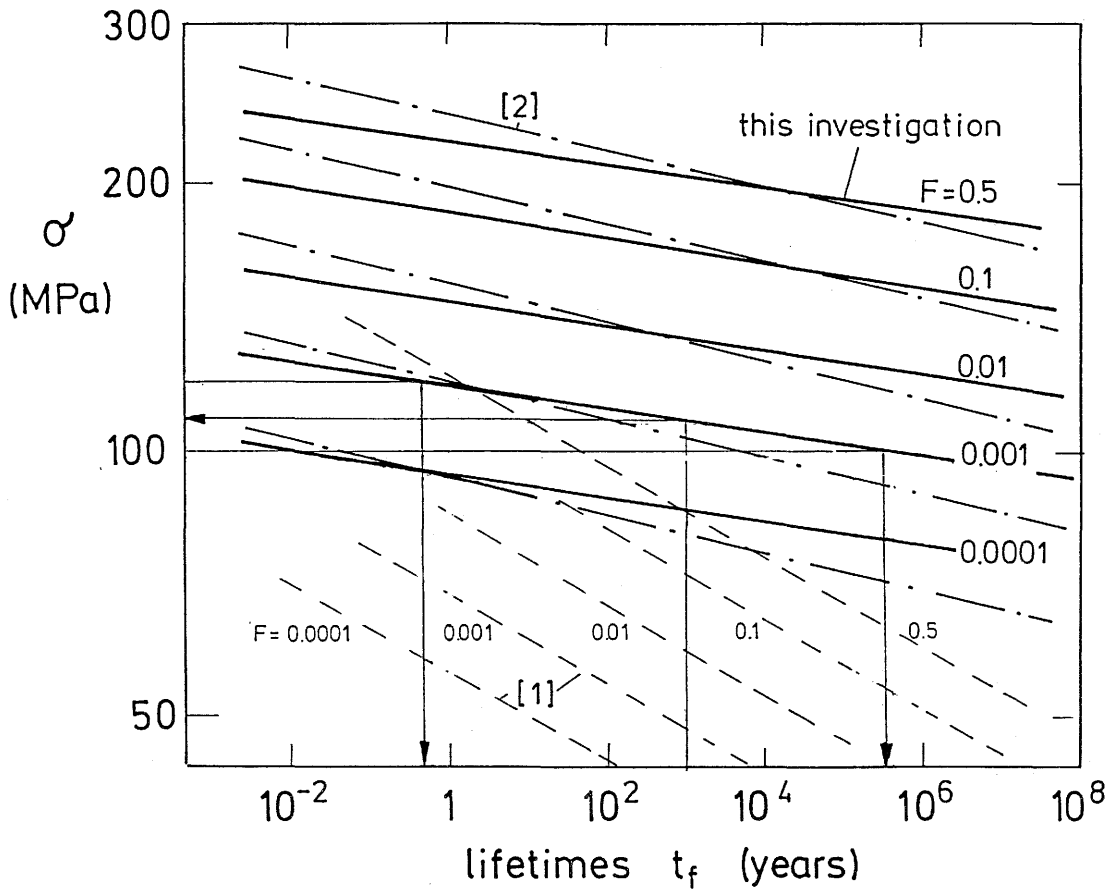


Fig.7 Nomograph for lifetime predictions:  
 (solid line: this investigation);  
 (dashed lines: material investigated in [1]);  
 (dashed-dotted lines: material investigated in [2]).

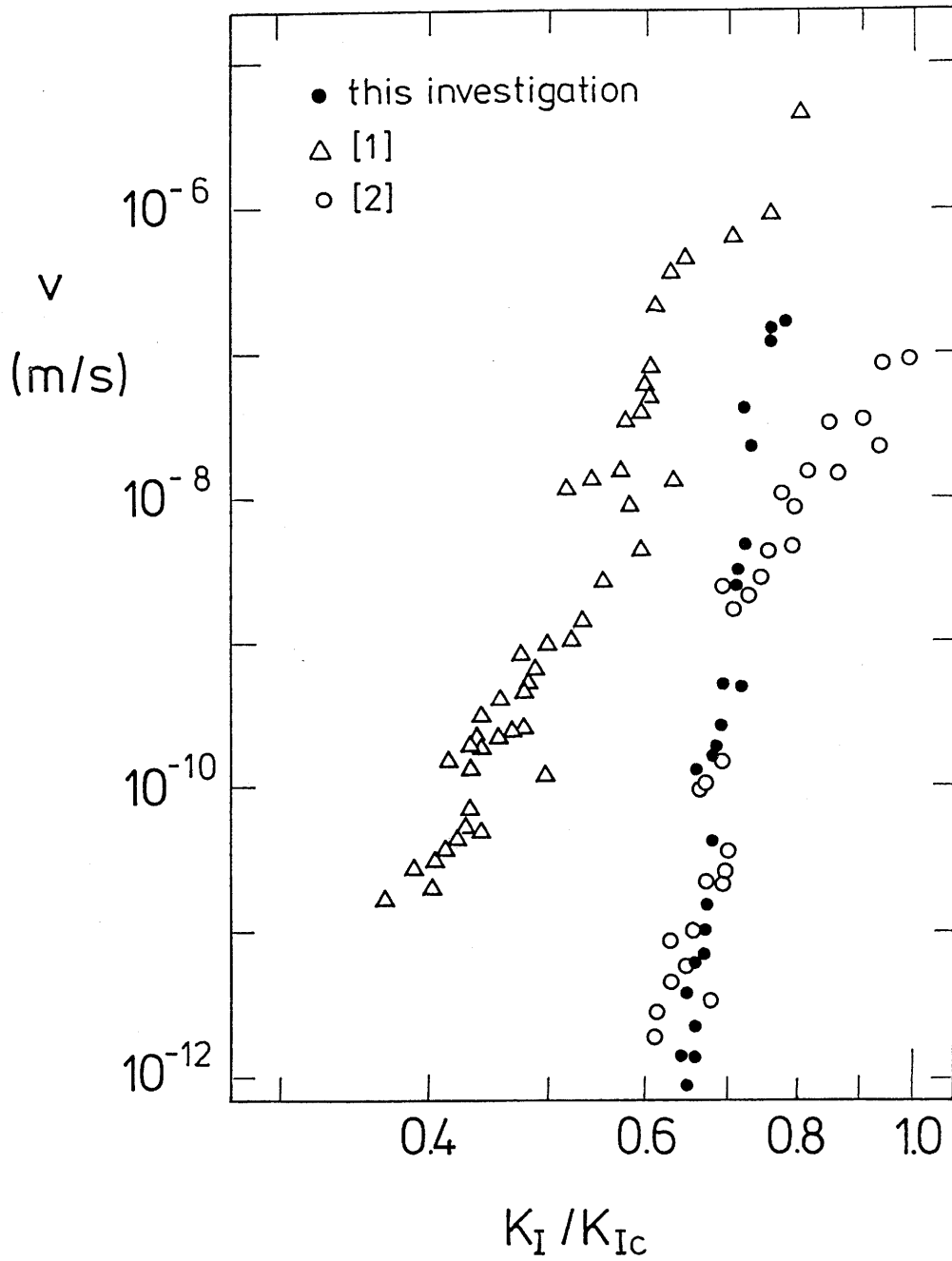


Fig.8 Comparison of subcritical crack growth behaviour of the competing aluminas.